Carbon Science

Vol. 4, No. 4 December 2003 pp. 168-174

Distribution of Silver Particles in Silver-containing Activated Carbon Fibers

S. K. Ryu♠, S. Y. Eom, T. H. Cho, and D. D. Edie*

Department of Chemical Engineering, Chungnam National University, Daejeon 305-764, Korea
*Center for Advanced Engineering Fibers and Films, Clemson University, Clemson, SC 29634, USA
♠e-mail: *skryu@cnu.ac.kr*
(Received December 6, 2003; Accepted December 15, 2003)

Abstract

Silver nitrate ($AgNO_3$) powder was mixed into a reformed pitch precursor. Then, the silver-containing pitch was melt spun to form round and "C" shape fibers. A wire mesh was inserted prior to the nozzle to improve the spinnability of the silver-containing precursor pitch. Silver particles in the carbon fibers (CFs) were detected by XRD and TEM. These tests showed that silver particles were uniformly distributed and the total amount of silver remained constant during stabilization and carbonization. Next, the silver-containing CFs were activated by steam diluted in nitrogen gas. Silver particles accelerated the activation rate, but the specific surface areas of the silver-containing ACFs were similar to those of non-silver containing ACFs at the same burn-off levels. The specific surface area of the C-shaped activated carbon fibers was larger than that of the round activated carbon fibers. The likely reason is that the surface area of a C-shaped CF is about two times larger than that of a round CF when equivalent cross-sectional areas are compared. A small amount of silver particles in the periphery of the CFs was removed during the activation, but the remainder of silver was stayed within the ACFs.

Keywords : *Activated carbon fibers, Spinnability, X-ray diffraction, Porosity, Specific surface area*

1. Introduction

Metal-containing carbon adsorbents including activated carbon fibers (ACFs) are being developed and evaluated for a variety of applications [1-3]. The metal-containing ACFs can be used not only as adsorbents but also as catalyst supports. Silver is one of the metals that is attracting particular attention because of its antibacterial activity [1, 4-10].

Oya *et al.* prepared silver-containing precursors by blending silver nitrate ($AgNO_3$) into phenolic resin [4] and silver acetate (CH_3COOAg) into isotropic petroleum pitch [5]. These precursors were melt spun into fibers and activated. After soaking in the flowing tap water for 20 days, the ACFs lost one-third of their initial silver content [4, 5]. Wang *et al.* prepared silver-containing ACFs by immersing ACFs in an aqueous solution of silver nitrate [8-10]. They found that silver particles blocked the pores, reduced the specific surface area [10], and rapidly washed out in flowing tap water [9].

In the previous work [11], the physical properties of silver-containing ACFs were studied. Silver particles were found to accelerate the activation rate, but the specific surface areas of silver-containing ACFs were found to be similar to those of non-silver containing ACFs. The average pore diameter of silver-containing ACF increased from 9.7 Å to 18.8 Å, but was still in micropore range. The previous work suggested that the silver content and its distribution in ACFs should be studied more carefully during spinning and activation. In subsequent work, we found that the spinnability of the silver-containing pitches could be improved by inserting a wire mesh distributor in the spinneret [12]. The C-shaped or non-circular CFs exhibit superior mechanical properties when compared to round CF [13, 14]. The external surface area of C-shaped CF is larger than that of round fiber with equivalent cross-sectional area. Therefore, one might expect that the C-shaped ACFs exhibit better properties than round ACFs.

The purpose of this study is to investigate the distribution of silver particles in round and C-shaped ACFs. The silver-containing precursor pitch was prepared by mixing silver nitrate to reformed petroleum pitch. Then the precursor pitches were melt spun into round and C-shaped carbon fibers at optimum spinning conditions. During the preparation of silver-containing CFs and ACFs, the amount of silver was measured by ICP for each step. Critical properties of silver-containing ACFs, such as specific surface area and pore size distribution, were measured. Also, the physical state and the distribution of silver particles in the ACFs were observed by TEM.

2. Experimental

Naphtha cracking bottom oil (SK oil, Korea) was reformed

at 390°C for 3 hours [11]. The softening point of the final reformed pitch was 240°C. The benzene and quinoline insoluble contents of the reformed pitch were 44.2 and 1.1 wt%, respectively. Silver nitrate ($AgNO_3$) powder was directly mixed to reformed pitches to prepare precursor pitches containing 0.1, 1.0, and 2.0 wt% silver. These silver nitrate-containing pitches were then ground in a homogenizer. The softening points of the precursor pitches were measured using a Mettler FP 800.

Melt-spinning was performed at temperatures ranging from 290°C to 330°C using a spinneret with a nozzle diameter of 0.5 mm for round CF (R-CF). An annular nozzle with an outer diameter of 1.8 mm and an inner diameter of 1.4 mm was used to melt spin the C-shaped carbon fibers (C-CF). A wire mesh distributor (50 microns) was inserted immediately prior to the spinneret to ensure uniform mixing of the precursor pitch and, therefore, enhance the spinnability. As the fibers emerged the nozzle, they were cooled by the surrounding air and collected by a takeup winder. The winding speed was constant for each trial, and fiber samples were produced at takeup speeds ranging from 1.2 to 9.7 m/s (the maximum speed of the winder). A microscope was used to measure the diameter of as-spun fibers.

The as-spun fibers were stabilized by heating them in air at 1°C/min to 290°C and then holding them at this temperature for 2 hours. The stabilized fibers were then carbonized by heating them in nitrogen surrounding at 10°C/min to 1000°C and holding them at this temperature for 30 min. Finally, the carbon fibers were activated at 900°C in a mixed atmosphere of steam and nitrogen (H_2O/N_2=0.50).

Silver particles in CFs and ACFs were detected by analyzing the X-ray diffraction patterns generated by Ni-filtered CuKα-radiation. The physical state and the distribution of silver particles were observed by TEM. SEM was also used to observe the surface of CFs and ACFs. The BET specific surface areas and pore size distribution (PSD) were determined from the adsorption of N_2 at 77 K (Micromeritics ASPS 2010). The actual amount of silver in the CFs and the ACFs was determined using an ICP emission spectroscope (JY-24).

3. Results and Discussion

3.1. Preparation of silver-containing round and C-shaped fibers

Fig. 1 shows the softening points of the silver-containing precursor pitches. Softening point increased as the silver content of the mixture increased. This trend should be expected because the melting point of silver nitrate is 390°C.

In the previous work, the spinning temperature of silver-containing precursor pitch was found to increase as silver nitrate content increased. Also, as the silver nitrate content increased, the precursor pitch became extremely difficult to melt-spin into fibers because the silver nitrate acted as an impurity. Oya *et al.* also found that it was difficult to melt spin silver-containing precursor pitches [5]. In the current work, a thin wire mesh distributor was used to homogenize the precursor pitch, and this modification greatly improved the spinnability.

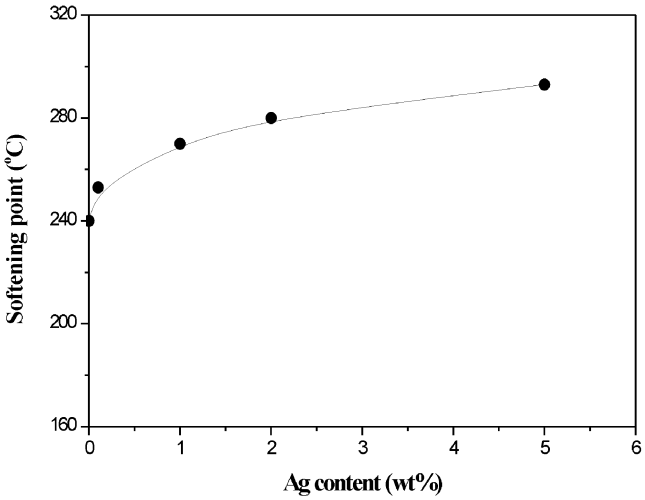

Fig. 1. Softening point of precursor pitch with respect to silver content.

The spinning temperature and spinnability of the precursor pitches tested in this study were listed in Table 1. In general, the melt-spinning temperature depends on the softening point of pitch and the spinneret hole shape and size. The melt spinning temperatures of the silver-containing precursor pitches were approximately 50°C higher than their softening points (which, in turn, increased with silver content). The optimum melt spinning temperature for the pure precursor pitch using C-shaped spinneret capillaries was 290°C. However, when round capillaries were used to melt spin the same pitch, the optimum temperature was 310°C. The optimum

Table 1. Spinning temperature and spinnability of precursor pitches

As-spun CF	Silver contents (wt%)	Spinning temperature (°C)	Spinnability
R-CF	0.0	310	Excellent
C-CF	0.0	290	Excellent
R-Ag-CF	0.1	315	Good
R-Ag-CF	1.0	320	Good
R-Ag-CF	2.0	330	Good
C-Ag-CF	0.1	295	Good
C-Ag-CF	1.0	300	Good
C-Ag-CF	2.0	310	Good

*Excellent: The length of CFs is longer than 12 m without breakage.
Good: The length of CFs is 6 m~12 m without breakage.
Poor: At least one breakage is happened in 6 m.

Table 2. The average diameter of R-CFs and C-CFs

Silver content (wt%)	R-CFs (μm)	C-CFs (μm)	
		External	Internal
0.0	20	36	26
0.1	28	44	28
1.0	34	51	30
2.0	36	52	30

melt-spinning temperature for the silver-containing pitches also differed 20°C, depending on whether the C-shaped or round capillaries were used.

There is no criterion on the level of spinnability of pitch spinning. Therefore, we suggested the criterion of spinnability as follows. Spinnability during each trial was classified as excellent, good, or poor. Excellent spinnability indicates that fibers longer than 12 m could be spun without breakage. Good spinnability implies that continuous fibers with lengths of between 6 and 12 m could be produced. Poor spinnability means that fibers could not be spun with lengths equal to or greater than 6m. Based on this criterion, the spinnability of the 2.0 wt% silver-containing precursor pitch was good, but the spinnability of the 5.0 wt% silver-containing precursor pitch was poor. In general, the spinnability of the precursor pitch decreased as the silver content increased. As one might expect, the spinnability of silver-containing precursor pitch improved as the takeup speed decreased. The average diameters of silver-containing as-spun fibers are listed in Table 2. Although the takeup speed could have been adjusted to melt spin each precursor into R-CFs with the same diameters, the objective of this study was to compare the adsorption characteristics of round and C-shaped carbon fibers with equivalent cross-sectional areas. Therefore, the takeup speed was controlled to yield R-CFs and C-CFs with similar cross-sectional areas. The diameters of these round and C-shaped fibers were constant along the fiber length. By comparison, the diameter of Oya's silver-containing fiber varied from 15 to 50 μm as a result of the poor spinnability [5].

The theoretical external surface areas of the as-spun round and C-shaped carbon fibers can be estimated using following equations:

Round CF:

$S_r = \pi LD$

C-shaped CF (assuming that the open angle of C-CFs is 120°):

$$S_c = \left(\frac{2\pi L}{3}\right)(D_o + D_i) + L(D_o - D_i),$$

where,

D = diameter of round CF

D_o = outer diameter of C-shaped CF

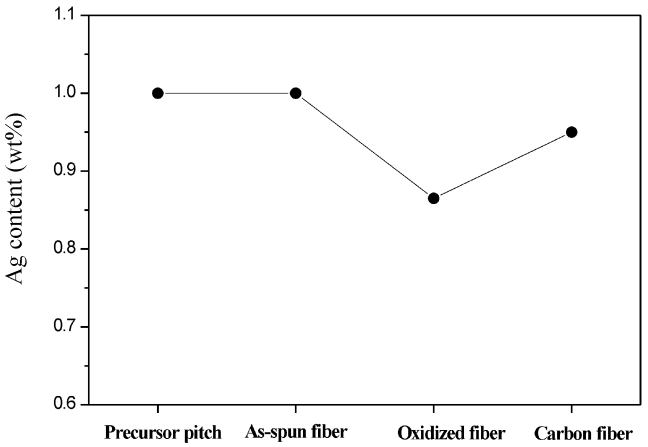

Fig. 2. Silver content change of 1.0 wt% silver-containing R-CF.

D_i = inner diameter of C-shaped CF

L = fiber length

If the average open angle of C-CFs is 120° and the cross-sectional area is the same as that of the R-CFs, the external surface area of C-shaped as-spun fiber will be about two times larger than that of round as-spun fiber.

3.2. Change of silver content during preparation of CFs

Fig. 2 shows the silver content change of 1.0 wt% silver-containing R-CF at various steps in the process. This relative change in silver content was caused by the addition or removal of oxygen and hydrogen during the stabilization and carbonization steps. The overall weight of both non- and 1.0 wt% silver-containing CFs increased about 12% during the stabilization step. However, weights of these same fibers decreased 25~30% during the carbonization step, depending on carbonization temperature. During the carbonization step the silver nitrate decomposed, yielding silver particles. The 2.0 wt% silver-containing C-CF showed similar changes in silver content. From the results, the amount of silver remains constant during the preparation of CFs, irrespective of the initial silver content and cross-sectional shape of the as-spun fiber.

Fig. 3 shows the relationship between silver content and carbonization temperature. During carbonization any remaining oxide functional groups were removed and unstable carbon was burned-off. As a result, the silver content increased as the carbonization temperature increased. The weight loss of carbon fiber rapidly increased as the temperature exceeded 1000°C, and this resulted in an increase in the silver content. However, at temperatures greater than 1200°C, the silver content rapidly decreased and the fibers became very fragile compared to the non-silver-containing CFs.

Fig. 4 shows the X-ray diffraction profiles of non-silver containing CF and 1.0 wt% silver-containing CFs. At a diffraction angle of 38°, Ag-peaks could be detected in silver-containing R- and C-CF, while no Ag-peak could be detected

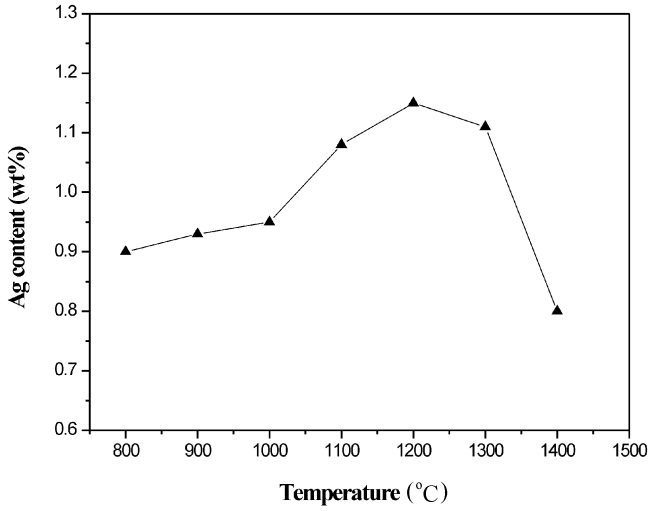

Fig. 3. Silver content change of 1.0 wt% R-CF with respect to carbonization temperature.

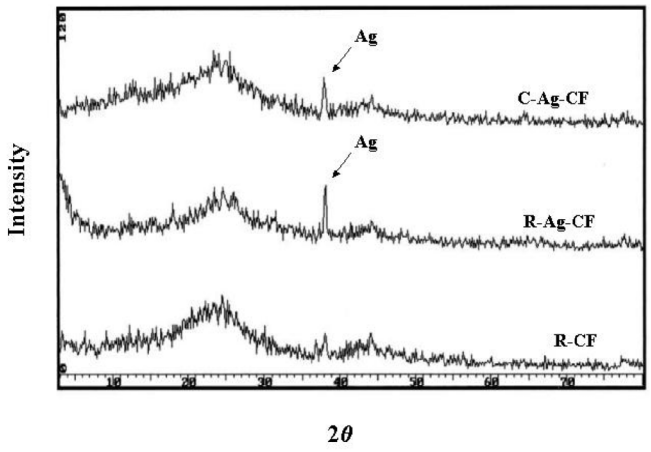

Fig. 4. X-Ray diffraction patterns of 1.0 wt% silver-containing R- and C-CF.

in the non-silver containing CFs. Oya *et al*. also reported the Ag-peaks at a 2θ of 38° [4], Since silver nitrate can not be observed by XRD, this indicates that the silver within the fibers exists as a free metal.

3.3. Activation of round and C-shaped CFs

The burn-off percent for round and C-shaped CFs are compared in Fig. 5. The burn-off of C-CF was larger than that of R-CF because of thinner limb thickness of the C-CF compared to the diameter of the R-CF and larger external surface area. The burn-off of silver-containing CF was greater than that of the non-silver-containing CF. Also, the burn-off increased as the silver content increased, indicating that silver particles accelerate the rate of activation. This supports the finding of others. Oya *et al.* found that silver-cobalt alloy particles can catalytically activate carbon fibers [1]. Thomas [15] also reported that Ag-metal executed rotary motion and

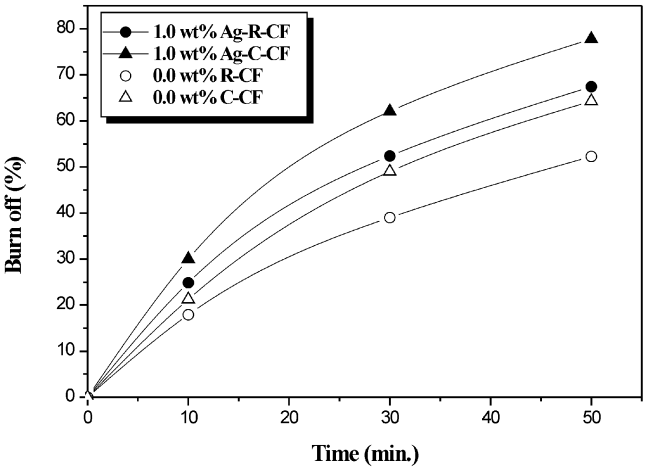

Fig. 5. Burn-off of R- and C-CFs with respect to time.

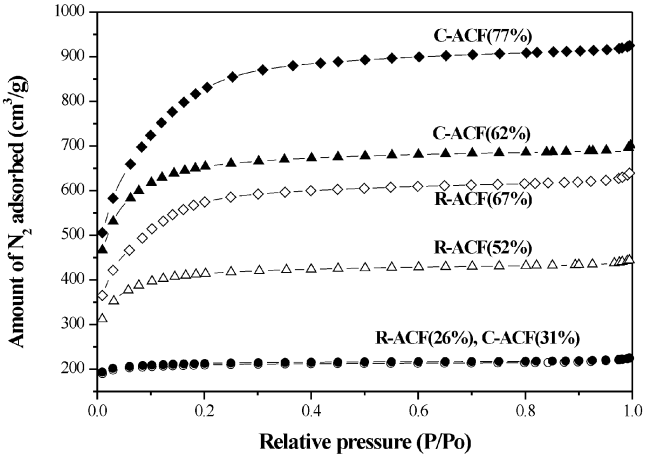

Fig. 6. N_2 adsorption isotherms of 1.0 wt% silver-containing R- and C-ACFs.

accelerated the rate of oxidation for graphite under inert gas such as N_2 or Ar when the temperature reaches to 700°C.

Fig. 6 shows the N_2 adsorption isotherms of 1.0 wt% silver-containing ACFs. All the isotherms are Type-I, which indicates that the pores developed in these ACFs are mainly micropores, even though silver particles accelerate the activation. The amount of nitrogen adsorption was proportional to the burn-off. As the figure shows, C-shaped ACFs exhibit greater nitrogen adsorption capacities than R- ACFs. This is most likely caused by the thin limb thickness and larger surface area of the C-ACFs.

Fig. 7 shows the variation in specific surface area with burn-off for the non-silver-containing and the 1.0 wt% silver-containing ACFs (both round and C-shaped). The specific surface area of C-ACFs, at any given value of burn-off, is larger than that of R-ACFs. However, the specific surface areas of silver-containing R-ACFs were similar to those of the non-silver-containing R-ACFs at similar burn-off levels, even though the silver-containing ACFs exhibited higher

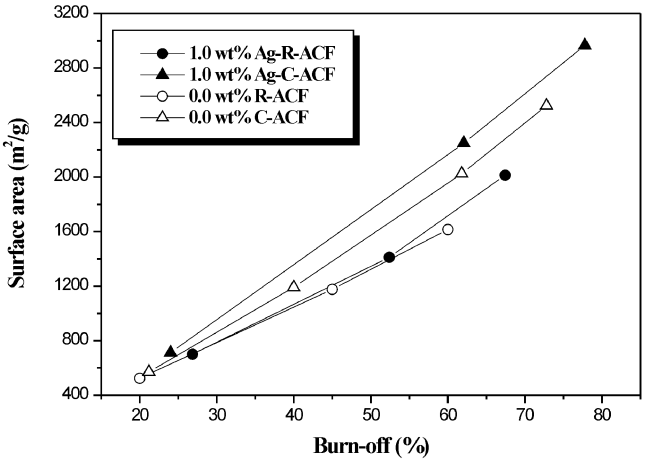

Fig. 7. Specific surface area of R- and C-ACFs with respect to burn-off.

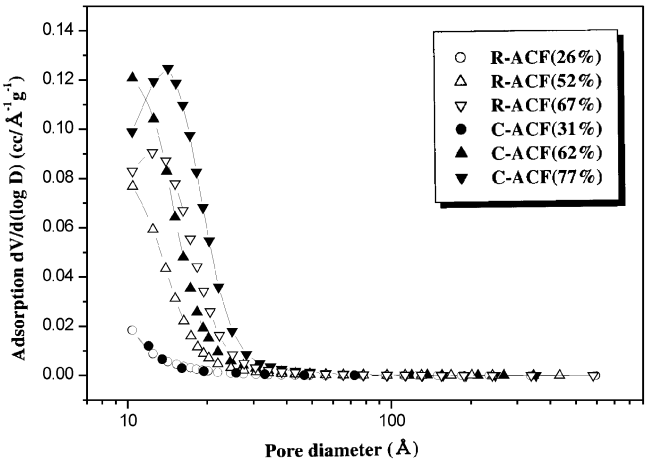

Fig. 8. Pore size distribution of 1.0 wt% silver-containing R- and C-ACFs.

activation rates. The specific surface area of 1.0 wt% silver, 77% burn-off Ag-C-ACF is about 3000 m^2/g, which is considerably greater than that reported by Oya (740 m^2/g, 0.63 wt% silver, 67% burn-off R-ACF [5], 1940 m^2/g, 2.2 wt% silver, 79% burn-off R-ACF [4]). This difference is the direct result of the precursors, fiber shapes and so on.

Fig. 8 shows the pore size distribution of 1.0 wt% silver-containing R- and C-ACFs. As the figure shows, the pore size appears to depend on burn-off, rather than on fiber shape. The average pore size increased with increasing burn-off for both R- and C-ACF. However, all the ACFs show an average pore size about 10~20 Å.

Fig. 9 shows SEM photos of the 1.0 wt% silver-containing CFs and ACFs. Some chips were observed on the surface in both silver-containing R- and C-CFs. However, it is difficult to observe silver particles directly in this figure. An analysis showed that these chips were caused the coalescence of some silver particles during the carbonization [11]. Use of

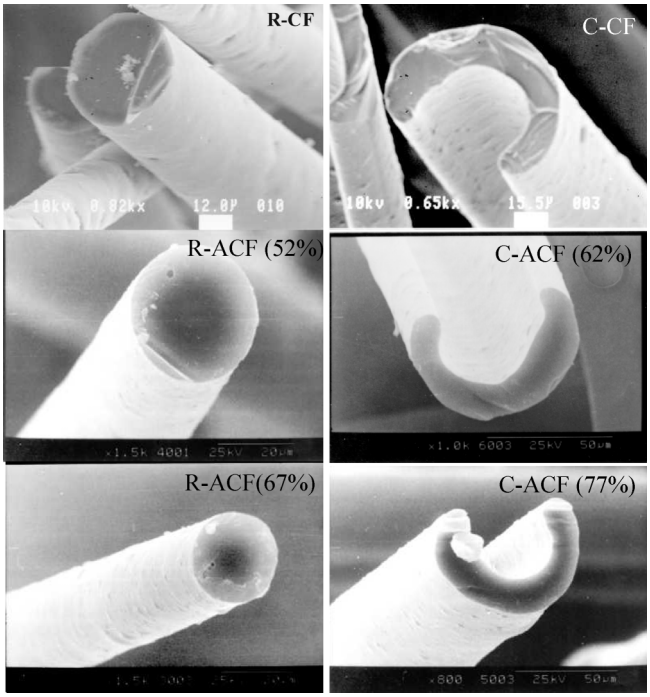

Fig. 9. SEM photos of 1.0 wt% silver-containing R- and C-ACFs.

the wire mesh distributor appeared to reduce the number of chips. Wang *et al.* reported that they could observe fine silver particles on the surface of ACF which was treated by vacuum impregnation in silver nitrate solution [9], however, could not observe silver particles on the surface of ACF supporting silver-loaded mesoporous molecular sieves [2].

3.4. Distribution of silver in ACFs

The XRD patterns of 1.0 wt% silver-containing C-ACFs are shown in Fig. 10. The Ag-peaks for the CFs and the ACFs appeared at the same 2θ value (38°), indicating that the silver particles did not change their physical state during

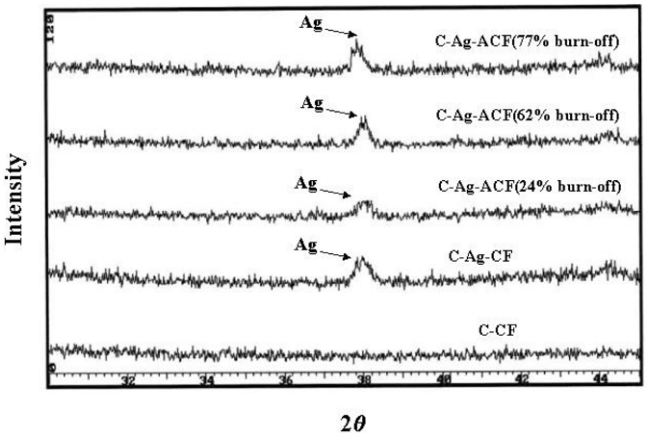

Fig. 10. X-Ray diffraction patterns of CFs and ACFs.

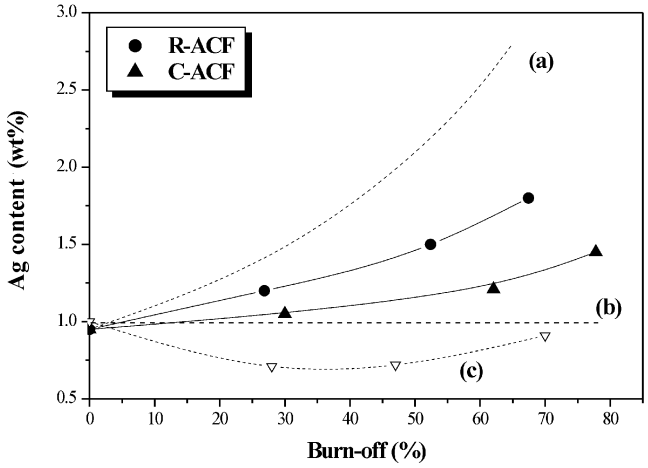

Fig. 11. Change of silver contents for 1.0 wt% R and C-ACFs during activation.

the steam activation. Oya reported that the intensity of the peak increased with as activation proceeded [4].

The distribution of silver particles in CFs and ACFs is extremely important. The silver particles must be uniformly distributed in the CF if ACFs with uniform pore structures are to be produced. Fig. 11 shows the change of silver content in 1.0 wt% R- and C-ACFs during burn-off. If only carbon is removed during the burn-off progress, the silver content should increase following dotted line (a). If carbon and silver particles are removed at equal rates during burn-off, the silver content should remain constant and follow dotted line (b). In our previous work [11], the majority of silver particles were located at outer region of the fiber and did not migrate into core during activation. Therefore, silver particles separated quickly from the fibers as the activation progressed, and the silver content followed dotted line (c). This indicated that the weight loss of the silver particles was larger than that of carbon. However, Oya *et al.* observed an increase of silver content, following the line (a) as activation proceeded and reported that there were no difference between measured and calculated values of silver content in phenolic resin based ACFs [4]. However, his calculation assumed that only carbon was burned-off. There was no indication that the silver particles migrated into the fiber core during activation. How could the silver content has increased without silver migration? One possible explain is that the most of silver particles were located in the core and easily aggregated to large size during the activation. On the other hand, they reported that silver-cobalt alloyed particles in the pitch based carbon fiber migrated into the fiber core, yielding channels as activation progressed [1]. The difference between Oya's earlier and latter results is likely the result of using cobalt and a different precursor.

In the present work, the silver content increased with increasing burn-off, following a trend between lines (a) and

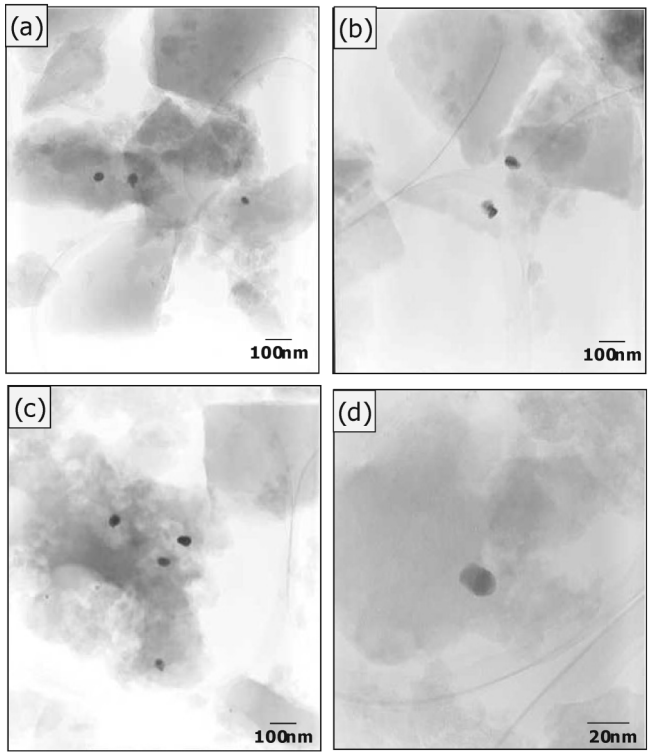

Fig. 12. TEM photos of 1.0 wt% silver-containing R- and C-ACFs.

(b), which differs from our previous result [11]. Only a small amount of silver particles in the periphery of the CFs was removed during the activation. The remainder stayed within the CFs and was distributed uniformly within the core region rather than outer region. The C-shaped CFs lost silver particles more easily than R-CFs because of thin limb thickness and their larger external surface area.

Fig. 12 shows TEM photos of silver particles in the CFs and the ACFs. The silver particles were dispersed rather uniformly in the fibers. The physical states and size of silver particles in ACFs were same as those in the CFs. The size of silver particles ranged from 15 to 30 nm, smaller than that reported in previous work [11]. Wang *et al.* reported that silver particles ranged from 50 to 350 nm [9]. Li *et al.* reported that silver particles ranging from 20 to 40 nm were found in the core of their ACFs whereas at the surface the size of the silver particles ranged from 20 nm to 1.5 μm [10]. They prepared the silver-containing ACF by immersing ACF in silver nitrate aqueous solution and then heating the fiber to 420°C. However, they did not explain how the silver particles in this size range can generate smaller micropores. Fig. 12 shows that there were no signs of coalescence or migration of silver particles in the ACFs. The figure confirms that the wire mesh immediately prior to the spinneret uniformly distributed the silver particles in the as-spun fibers, and the distribution maintained uniform in the ACFs.

4. Conclusions

Inserting a wire mesh distributor immediately prior to the nozzle dramatically improved the spinnability of the silver-containing precursor pitch. Total silver content of the carbon fibers was constant during oxidation and carbonization. The silver particles existed as free metals in the carbonized fibers. Silver particles accelerated the activation rate, but the specific surface areas of the silver-containing ACFs were similar to those of non-silver containing ACFs at the same burn-off levels. A small amount of silver particles in the periphery of the CFs was removed during the activation, but the remainder of silver was uniformly stayed within the ACFs. The size of the silver particles does not change during the activation step. The C-shaped ACFs exhibit larger specific surface area than round ACFs because of their larger external surface area.

Acknowledgments

The authors wish to acknowledge the financial support from KOSEF (Korea Science and Engineering Foundation) and NSF (National Science Foundation of U.S.A.) for this work (F01-2000-000-20045-0).

References

[1] Oya, A.; Yoshida, S.; Alcaniz-Monge, J.; Linares-Solano, A. *Carbon* **1996**, *34*(1), 53.
[2] Wan, Y. Z.; Wang, Y. L.; Cheng, G. X.; Luo, H. L.; Dong, X. H. *Carbon* **2001**, *39*(10), 1607.
[3] Oya, A.; Yoshida, S.; Alcaniz-Monge, J.; Linares-Solano, A. *Carbon* **1995**, *33*(8), 1085.
[4] Oya, A.; Yoshida, S.; Abe, Y.; Iizuka, T.; Makiyama, N. *Carbon* **1993**, *31*(1), 71.
[5] Oya, A.; Wakahara, T.; Yoshida, S. *Carbon* **1993**, *31*(8), 1243.
[6] Oya, A.; Banse, T.; Ohashi, F.; Otani, S. *Appl. Clay Sci.* **1991**, *6*, 135.
[7] Oya, A.; Banse, T.; Ohashi, F. *Appl. Clay Sci.* **1992**, *6*, 311.
[8] Wan, Y. Z.; Wang, Y. L.; Wen, T. Y. *Carbon* **1999**, *37*(2), 351.
[9] Wang, Y. L.; Wan, Y. Z.; Dong, X. H.; Cheng, G. X.; Tao, H. M.; Wen, T. Y. *Carbon* **1998**, *36*(11), 1567.
[10] Li, Ch. Y.; Wan, Y.; Wang, Y. L.; Jiang, X.; Han, L. M. *Carbon* **1998**, *36*(1), 61.
[11] Ryu, S. K.; Kim, S. Y.; Gallego, N.; Edie, D. D. *Carbon* **1999**, *37*(10), 1619.
[12] Cho, T. H.; Eom, S. Y.; Ryu, S. K. Extended Abstracts 26th Conference on carbon material. Nagano, Japanese Carbon Society, **1999**, 266-267.
[13] Ryu, S. K.; Yang, X. P.; Lu, Y. F. *Carbon Science* (Korea), **2000**, *1*(3), 165.
[14] Edie, D. D.; Fox, N. K.; Barmett, B. C.; Fain, C. C. *Carbon* **1986**, *24*(4), 477.
[15] Thomas, J. M. "*Chemistry and Physics of Carbon*", Vol. 1, ed. P. L. Walker, Jr., Marcel Dekker, New York, 1965, 189.